20th International Conference on Structural Mechanics in Reactor Technology (SMiRT 20)
Espoo, Finland, August 9-14, 2009
SMiRT 20-Division I, Paper 1654

Tensile and toughness properties for the RSE-M Code

Patrick Le Delliou[a], Bruno Barthelet[b], Aurore Parrot[a], Lionel Sainton[a], Marc Berveiller[a], and Sébastien Saillet[a]

[a]*Electricité de France, R&D Division, Moret-sur-Loing, France, e-mail: patrick.le-delliou@edf.fr*
[b]*Electricité de France, Nuclear Generating Division, Saint-Denis, France*

Keywords: Stainless steel, carbon-manganese steel, tensile properties, toughness, dynamic strain ageing

1 ABSTRACT

The RSE-M Code provides the essential rules and requirements for in-service inspection of pressure retaining components of the French NPP. Its scope is close to the scope of ASME B&PV Code Section XI Division 1, except that concrete components and metallic liners are not included.

The Code includes a procedure for determining the acceptability of flaws that have been detected by in-service inspection. The procedure is based upon the principles of fracture mechanics (LEFM and EPFM) and applies to ferritic and austenitic materials of the main components and piping. It makes use of partial safety factors on loading and material mechanical properties, so these properties must rely on a statistical approach. Yield strength and ultimate tensile strength 5% fractiles and dimensionless reference true stress-strain curves are provided by the Code for base metals and welds. For piping materials, the 16% fractiles of $J_{0.2mm}$ and J-Δa curves were codified. Mean values and standard deviations are given for fatigue crack growth rates for the main materials.

Between 2004 and 2006, a project was conducted by EDF to improve RSE-M Code flaw evaluation and to reduce unnecessary conservatisms. One objective of this project was to better understand the effects of aging and to improve the statistical analysis of the databases from experimental fracture mechanics programs on austenitic stainless steel piping and carbon-manganese ferritic steel piping and associated welds.

The results of this project have been processed to add or to improve statistical characteristic values in the next RSE-M Code edition. The new values are generally higher than the former values.

2 INTRODUCTION

The RSE-M Code (1997) provides the essential rules and requirements for in-service inspection of pressure retaining components of the French NPP (Faidy, 2000). The RSE-M code includes a procedure for determining the acceptability of flaws that have been detected by in-service inspection. The procedure is based upon the principles of fracture mechanics (LEFM and EPFM) and applies to ferritic and austenitic materials of the main components (Le Delliou, 2004). It makes use of partial safety factors on loading and material mechanical properties, so these properties must rely on a statistical approach.

Since 1995, several studies have been performed by AREVA NP and EDF to improve the knowledge of mechanical properties of the PWR materials and to determine statistical characteristic values used with corresponding safety factors in the flaw acceptance criteria (Barthelet, 1999). A significant sample of main component parts and welds was selected out of the 58 French PWR and the results of manufacturing test coupons were collected in databases. Data for reactor pressure vessels, steam generators, pressurizers, austenitic stainless steel piping and ferritic steel piping were statistically analyzed. The standard deviations of the tensile properties for each type of material appear to be rather small. Yield strength and ultimate tensile strength 5% fractiles and dimensionless reference true stress-strain curves are provided by the Code for base metals and welds. Because fracture mechanics properties are not measured during manufacturing, laboratory test results were used to estimate characteristic values or to establish correlations between manufacturing test coupons data and fracture mechanics properties. For piping materials, the 16% fractiles of $J_{0.2mm}$ and J-Δa curves were codified using the relationship $J_{\Delta a} = C\Delta a^{n}$.

Between 2004 and 2006, a project was conducted by EDF to improve RSE-M Code flaw evaluation and to reduce unnecessary conservatisms (Le Delliou, 2007). One objective of this project was to better understand the effects of aging and to improve the statistical analysis of the databases from experimental fracture mechanics programs on austenitic stainless steel piping and carbon-manganese ferritic steel piping and associated welds. For austenitic stainless steel welds, the effects of thermal aging on fracture toughness were better determined. Fracture toughness tests were conducted at different temperatures, on aged welds from different weld processes, including gas tungsten-arc weld. For carbon-manganese steels, the effects of strain aging on tensile properties and fracture toughness were studied by fracture toughness tests and theoretical models. Correlations were developed for estimating fracture toughness, tensile properties of carbon-manganese steel from material information of acceptance reports as sulfur content, aluminum content or upper shelf Charpy impact energy.

This paper recalls the main results of this project, concerning the experimental program, statistical analyses, correlations between properties and study of the strain aging phenomenon. The project involved the following materials:

- austenitic stainless steels (mainly welds),
- carbon-manganese steels (base metal and welds).

3 AUSTENITIC STAINLESS STEELS

3.1 Experimental program

A full-scale mockup of a narrow gap gas tungsten arc (GTA) weld between a 316L safe end and a 304L forged pipe was studied. Table 1 gives the chemical composition of the safe end and the weld. The ferrite content of the weld ranges between 8.1 % (root passes) to 11 % (last passes).

Table 1. Chemical composition (weight %) of the 316L base metal and the weld.

Product #	Material	C	Mn	Si	S	P	Cr	Ni	Mo	N
Base metal	**316L**	0.029	1.76	0.55	<0.003	0.022	17.49	12.25	2.33	0.063
GTA weld	**316L**	0.015 0.011	1.60 1.60	0.78 0.81	0.009 0.011	0.021 0.022	18.68 18.69	12.47 12.43	2.19 2.19	- -

The program included the following tests:

- tensile tests on specimens taken either in the axial direction (base metal) or in the circumferential direction (weld),
- Charpy impact tests on Charpy-V specimens taken in the axial-circumferential orientation (weld only),
- ductile fracture tests on CT specimens taken in the axial-circumferential orientation (base metal and weld).

The effect of thermal aging was investigated on the weld. Four thermal ageing conditions, 10,000 h at 350°C and 400°C, 30,000 h at 300°C and 350°C, were selected.

3.2 Experimental results

The results of the tensile tests on the GTA weld at room temperature and at 300°C are shown graphically on Fig. 1. The solid symbols correspond to the ultimate strength (labeled Rm) and the open symbols correspond to the 0.2 % yield strength (labeled Rp0.2). The thermal aging, especially at 400°C, increases the ultimate strength while the yield strength is unchanged. The specimens machined in the root passes of the weld have higher ultimate strength and yield strength values.

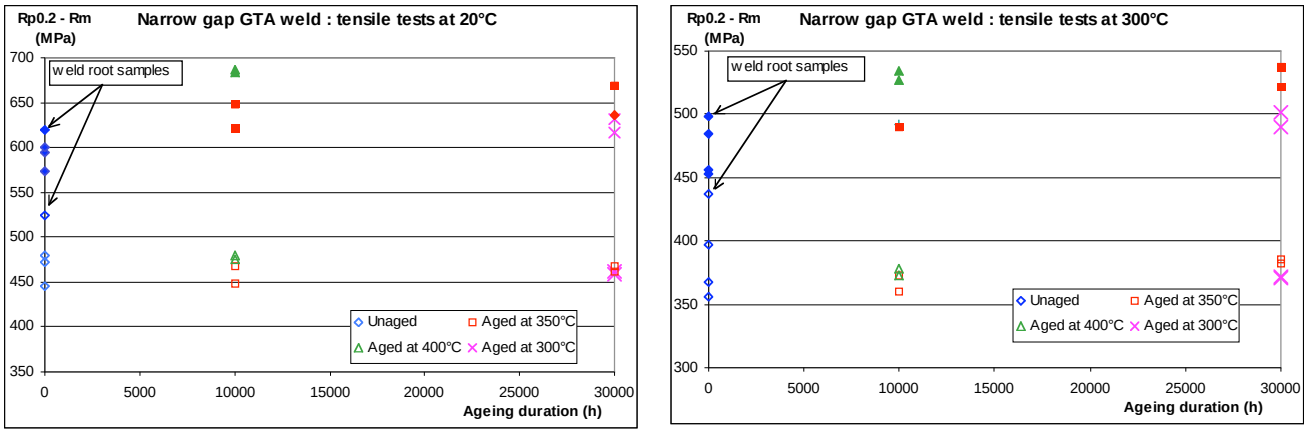

Figure 1. Effect of the thermal aging on the tensile properties of the GTA weld.

Regarding the effect of the thermal aging on KCV impact energy values, there is no clear effect at room temperature. At 300°C, the values in the un-aged condition are higher that the values obtained after ageing, with a large scatter. It was not possible to explain this scatter by the various locations of the specimens in the weld.

Fig. 2 shows the effect of the thermal ageing on fracture toughness properties at 20°C and 300°C for the GTA weld: the initiation fracture toughness $J_{0.2}$ (left figure) and the crack propagation resistance dJ/da (right figure). The tests were made on CT25 (25 mm thick) and CT40 (40 mm thick) specimens by the multiple specimen method. The decrease of the $J_{0.2}$ value due to the thermal aging is moderate. The same observation is made for the dJ/da parameter, except for the very high value at room temperature in the un-aged condition (700 MPa). This may be partially explained by the large scatter between specimens observed during the tests. Finally, fracture toughness tests were conducted on CT40 specimens taken in the 316L base material (LC orientation). Very high values of J were obtained, exceeding the J_{max} value allowable by the test standard:

- At room temperature: $J_{0.2}$ = 1891 kJ/m^2, dJ/da = 859 kJ/m^2,
- At 300°C: $J_{0.2}$ = 1170 kJ/m^2, dJ/da = 538 kJ/m^2.

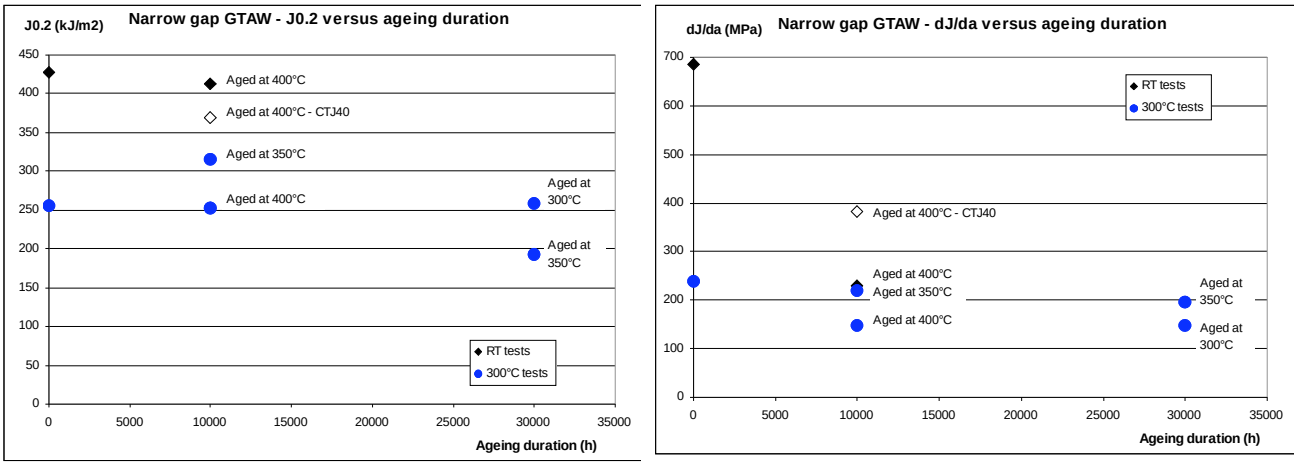

Figure 2. Effect of the thermal aging on the fracture toughness properties of the GTA weld.

3.3 Statistical analyses

The weld metal fracture toughness database used in 1996 to develop the $J_{0.2}$ values and J-Δa curves provided in Appendix 5.6 of the RSE-M Code was enriched by new results and corrected. A distinction was made between the welding processes, distinguishing SMAW (shielded metal arc welding) and SAW (submerged arc welding) on one side and GTAW on the other side. For each welding process, data were divided into four classes, according to the test temperature (T ≤ 100°C or T ≥ 200°C) and to the possible thermal ageing applied (with or without).

For each sample, a lognormal distribution law was chosen (a goodness-of-fit test having shown that it is the most pertinent distribution law) to calculate the 16% fractile. Moreover, to take into account the size of

the sample, the procedure of the ISO 16269-6 standard (2005) for establishing tolerance intervals was used (one-sided statistical tolerance limit factor k_3). Table 2 summarizes the results. For the SMAW and SAW welds, the values obtained with the un-aged data at T ≤ 100°C are slightly higher than the codified values. However the values for the other cases (aged data and un-aged data at T ≥ 200°C) are slightly lower than the codified ones, due to the factor k_3. For the GTAW welds, the size of the sample is small especially in the un-aged condition, so it was decided to codify in the RSE-M the values of the combined sample (aged and un-aged) for this condition.

Table 2. Results of the statistical analysis on $J_{0.2}$ values for 316L weld metal.

$J_{0.2}$ (kJ/m^2) 16% fractile	**SMAW and SAW**		**GTAW**	
	RSE-M Code	This study	This study	This study (*)
T ≤ 100°C - unaged	83	118	186	192
T ≤ 100°C - aged	67	58	169	
T ≥ 200°C - unaged	48	44	198	158
T ≥ 200°C - aged	38	36	136	

(*) without distinction between aged and un-aged data.

3.4 Correlations between properties

Instead of using lower bound values for the fracture toughness properties, a more accurate solution is to use a correlation between a measured property and the desired property. Fig. 3 and 4 show an example of correlation between the fracture toughness parameters $J_{0.2}$ and dJ/da and the KCV impact energy for the stainless steel welds, respectively at 20°C and around 300°C. On these figures, the red symbols are experimental values coming from Gavenda (1996), which are tests made on SMAW with 308 type filler metal.

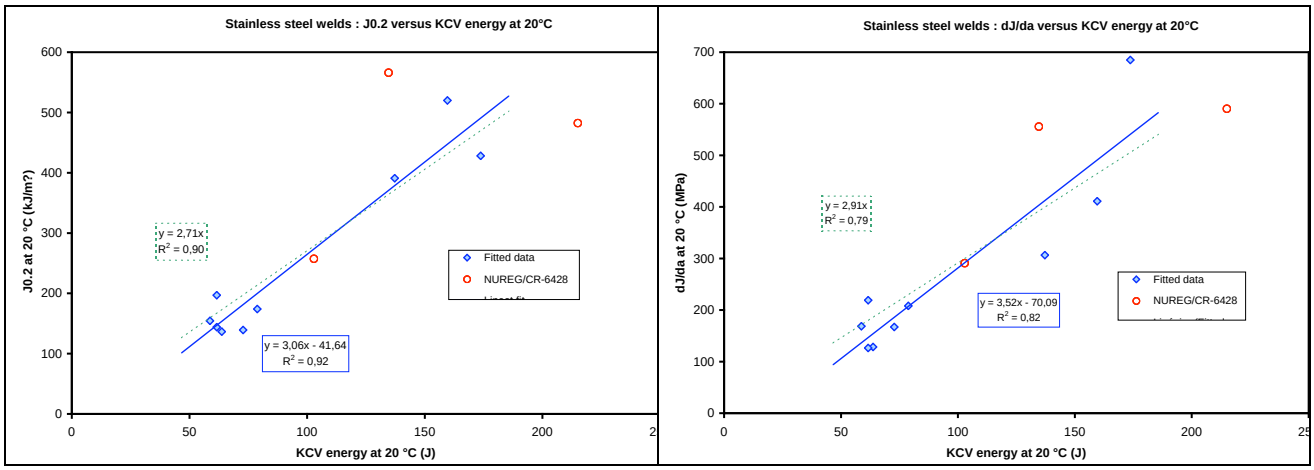

Figure 3. Stainless steel welds : $J_{0.2}$ and dJ/da versus KCV impact energy at 20°C.

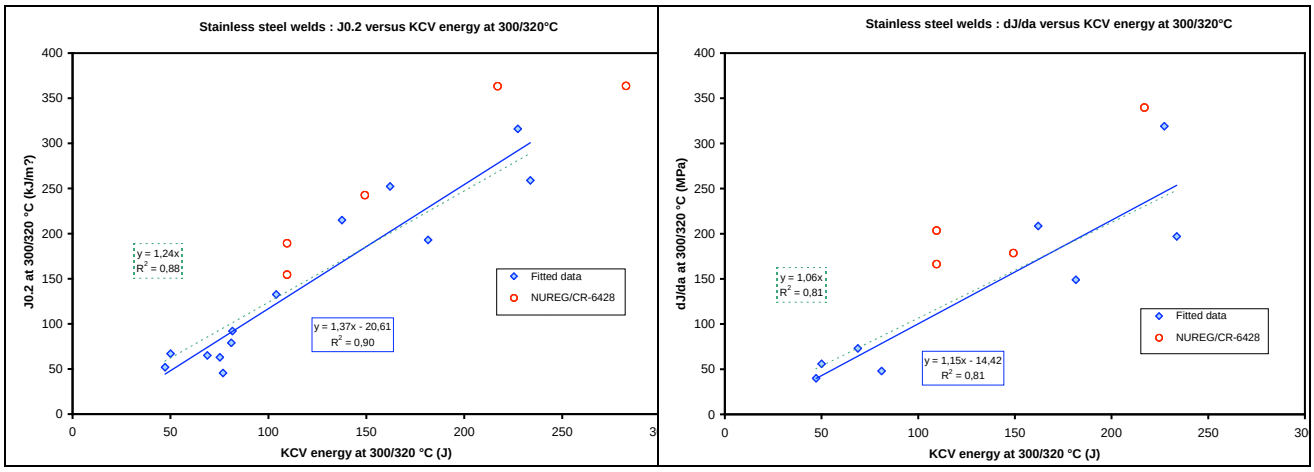

Figure 4. Stainless steel welds : $J_{0.2}$ and dJ/da versus KCV impact energy at 300/320°C.

4 CARBONE-MANGANESE STEELS

4.1 Experimental program

Four piping components have been used for this study. U631 and U634 are seamless pipes, whose French standard AFNOR designation is TU48C. U632 is a pipe with a longitudinal seam weld, made from a plate (AFNOR designation A48CP). U786 is a welded elbow withdrawn from service. Its exact material designation is unknown (either A42 or A48). Table 3 gives the chemical composition of these steels. Material U786 has the highest sulfur content (0.020 %), whilst U634 has the lower Al/N ratio, so it should be the most sensitive to strain aging.

Table 3. Chemical composition (weight %) of the base metals.

Product #	Material	C	Mn	Si	S	P	N	Al	Al/N
U631	**TU48C**	0.161	1.29	0.22	0.002	0.013	0.011	0.025	2.27
U632	**A48CP**	0.203	1.33	0.29	0.004	0.022	0.0051	0.037	7.25
U634	**TU48C**	0.19	1.07	0.27	0.0074	0.011	0.011	0.0085	0.77
U786	**A42 or A48**	0.20	1.15	0.24	0.020	0.016	0.005	0.030	6.00

Circumferential butt welds were made on pipes U631, U632 and U634, the latter containing three welds (labeled S1, S2 and S3). Table 4 lists the main characteristics of these welds. The welds U634 S2 and U634 S3 were fabricated with the same rod and flux batches. Due to the lack of space, the chemical composition of these welds will not be recalled here (see Le Delliou (2007)). The weld U631 has the highest sulfur and phosphorus contents, whilst U634 S1 has a low Al/N ratio and was selected for strain aging studies.

Table 4. Main characteristics of the pipes and the circumferential butt welds.

Pipe #	Diameter (mm)	Thickness (mm)	Weld designation	Type of weld	Stress-relieve
U631	762	41	Q71/849	SAW	Yes
U632	762	38	Q71/641	SMA	Yes
U634	457	38.7	Q71/841 S1	SMA	Yes
			Q71/842 S2	SAW	Yes
			Q71/843 S3	SAW	No

The program included the following tests:

- tensile tests on specimens taken in the axial direction,
- Charpy impact tests on Charpy-V specimens taken in the axial-circumferential (LC) orientation,
- ductile fracture tests on CT specimens taken in the axial-circumferential (LC) orientation.

The effect of thermal ageing was investigated on pipe U632 and weld U631, materials with the highest phosphorus content. Two thermal ageing conditions, 10,000 h at 350°C and 400°C, were selected. The effect of static strain aging was investigated on weld U634 S1, by applying a compressive cold work (two levels: 5 % and 11 %) before machining the specimens.

4.2 Experimental results

The results of the tensile tests for the pipes U631 and U634 are shown graphically in Fig. 5. The ultimate strength (noted Rm) of pipe U634 reaches a maximum at 300°C, while that of pipe U631 varies more smoothly with the temperature. The percentage reduction of area (noted Z %) of pipe U631 decreases steadily with the temperature, while that of pipe U634 reaches a minimum at 250°C. The pipe U634 appears a little more sensitive to DSA (Dynamic Strain Aging) than the pipe U631. No clear effect of the thermal ageing was evidenced on the tensile tests.

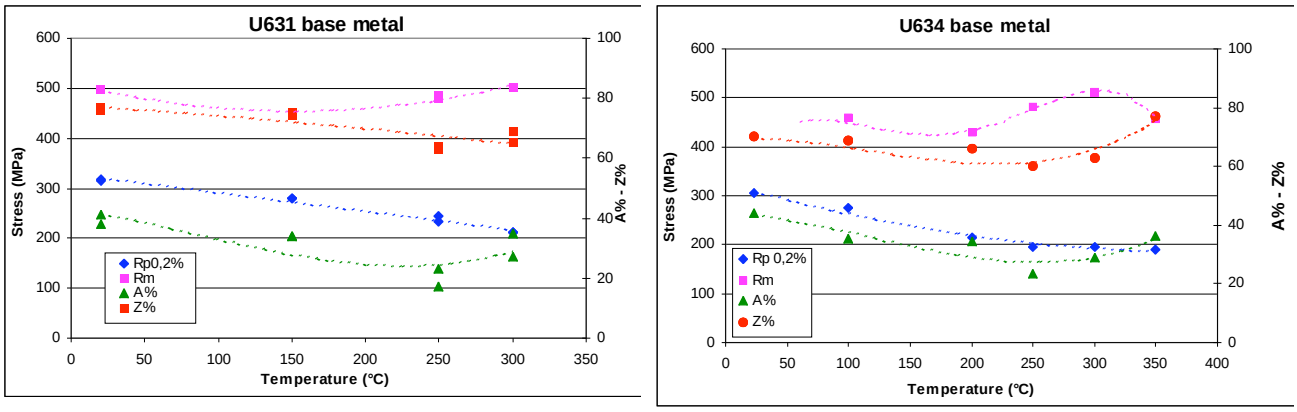

Figure 5. Temperature dependence of the tensile characteristics for the pipes U631 and U634.

Fig. 6 shows the effect of the thermal aging on impact energy curves for U632 base metal and U631 weld metal. The effect is noticeable only for the U631 weld metal at the highest ageing temperature (400°C), with a shift of 41°C of the TK7 temperature (temperature whose impact energy is 7 daJ/cm^2). Fig. 7 shows the effect of the static strain ageing on the U634 S1 weld metal. There is a shift towards higher temperatures for the impact energy curves (left figure) and for the percentage of cleavage fracture (right figure). It corresponds to an increase of about 10°C of the FATT (fracture appearance transition temperature) between the initial state (labeled ER) and the 5% cold work, and between the 5 % and the 11 % cold work.

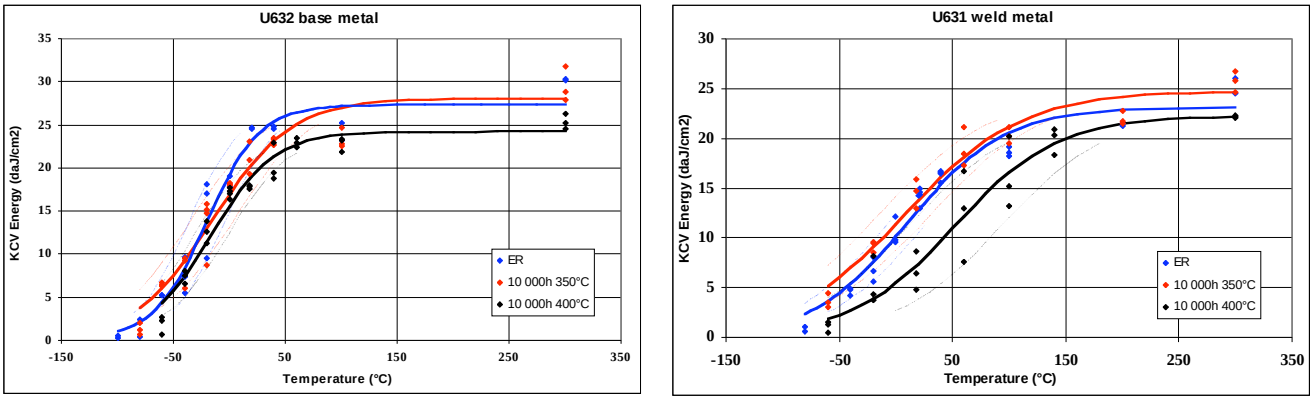

Figure 6. Effect of thermal aging on impact energy curves for U632 base metal and U631 weld metal.

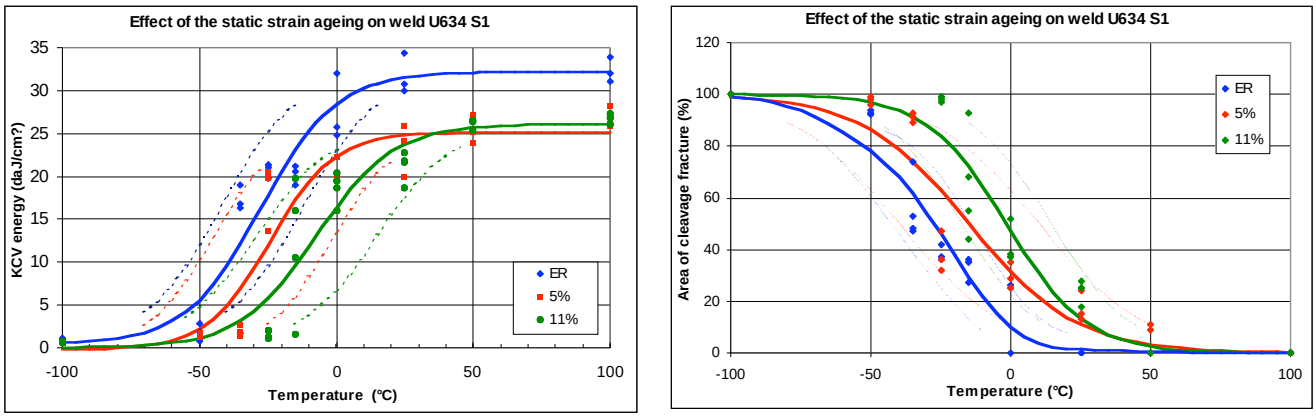

Figure 7. Effect of the static strain aging on U634 S1 weld metal.

Fig. 8 presents the upper shelf energy (USE) as a function of the sulfur content for all the products (solid symbols for the base metal and open symbols for the weld metal). For the base metal, a clear decrease of the USE as a function of the sulfur content is observed. For the weld metal, the USE values are higher than for the base metal and the dependence of these values to the sulfur content is less marked. This may be due to the shape of the manganese-sulfur particles, more globular in the welds.

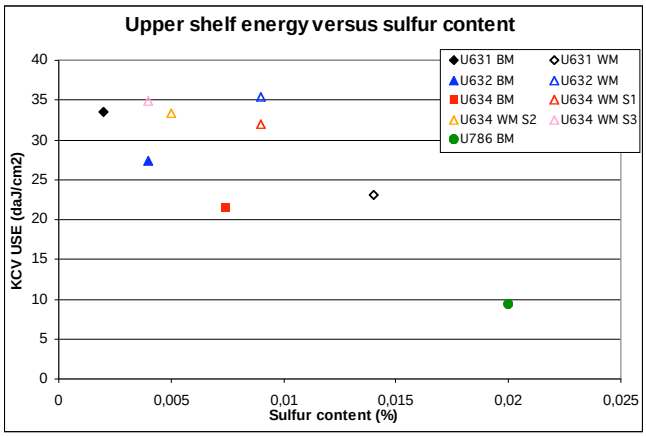

Figure 8. Upper shelf energy (USE) versus sulfur content.

Fig. 9 shows the results of the ductile fracture tests on the CT specimens for the base metals. The left-hand figure illustrates that the temperature dependence of the initiation fracture toughness $J_{0.2}$ can be very different according to the materials: U631 values decrease very much whereas U632 values stay constant. For the U634 base metal, the right-hand figure shows the evolution of $J_{0.2}$ and dJ/da (crack propagation resistance) versus temperature. Both parameters reach a minimum at around 200°C, which is typical of the dynamic strain aging effect. Fig. 10 (left-hand side) shows that the thermal aging has no significant effect. Fig. 10 (right-hand side) shows that the sulfur content has a strong effect on the $J_{0.2}$ values.

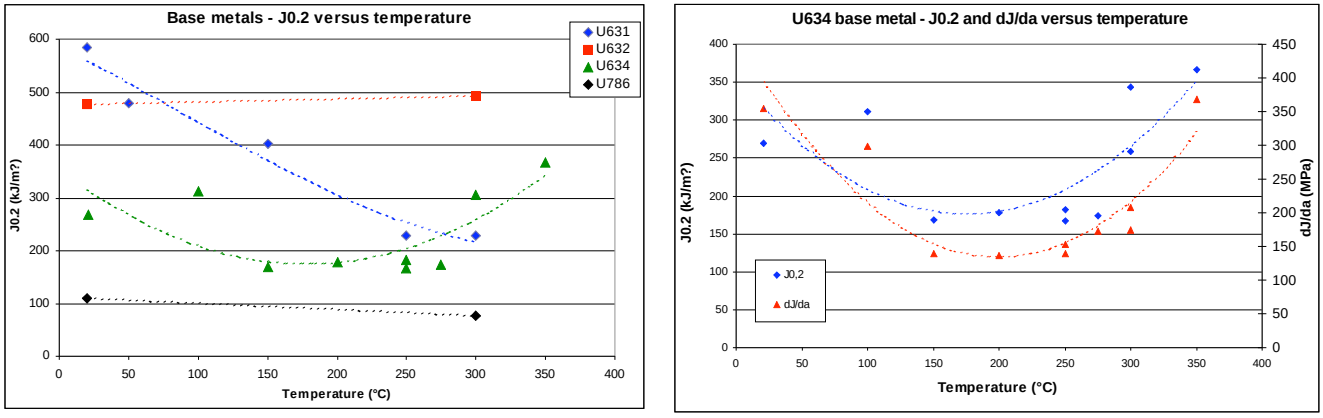

Figure 9. Results of the ductile fracture tests on CT specimens (base metal).

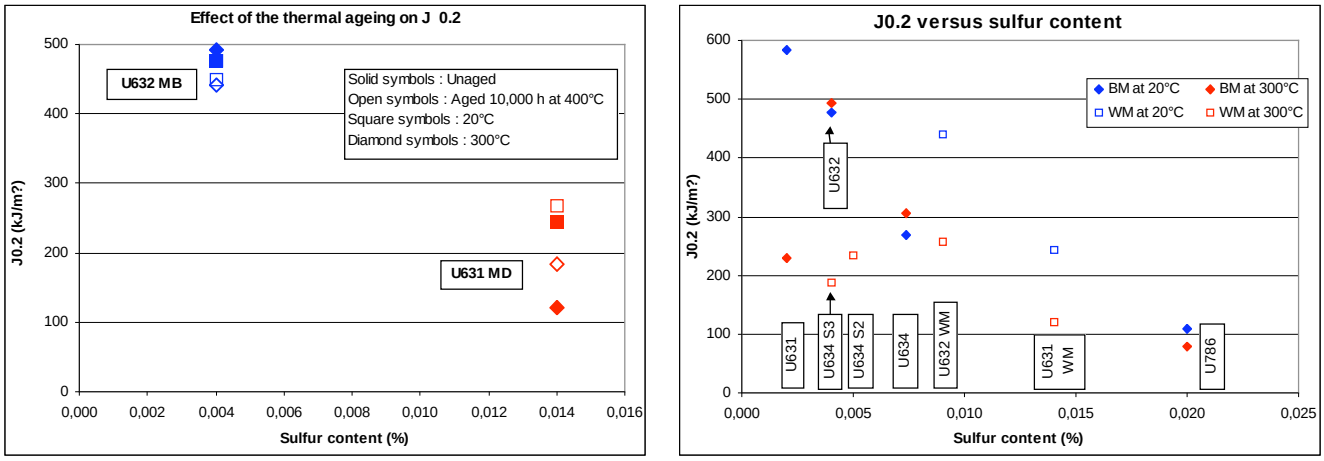

Figure 10. Results of the ductile fracture tests on CT specimens: effects of thermal aging and sulfur content.

4.3 Statistical analyses

The base metal and weld metal fracture toughness database used in 1996 to develop the $J_{0.2}$ values and J-Δa curves provided in Appendix 5.6 of the RSE-M Code was enriched by new results and corrected. For the base metal, a distinction was made between the specimen orientation (LC or CL, equivalent respectively to LT and TL on a plate). For each orientation, data were divided into two classes, according to the test temperature (T ≤ 140°C or T > 140°C). Moreover, for the LC orientation, the size of the sample was large enough to be divided into three classes, according to the sulfur content (S < 0.005 % - 0.005 % ≤ S ≤ 0.015 % - S < 0.015 %). For the weld metal, no distinction was made on the specimen orientation (all the specimens are machined in the TL orientation, respective to the weld joint) neither on the sulfur content (the range of the sulfur content of the database is not very wide). Hence, weld data were divided into two classes, according to the test temperature (T ≤ 140°C or T > 140°C).

For each sample, a lognormal distribution law was chosen (a goodness-of-fit test having shown that it is the most pertinent distribution law) to calculate the 16% fractile. Moreover, to take into account the size of the sample, the procedure of the ISO 16269-6 standard (2005) was applied. Table 5 summarizes the results. For the base metal with the CL orientation, the values obtained in this study are slightly lower than the codified values. This slight decrease is explained by the correction of some erroneous values and by the small size of the sample which increases the statistical tolerance limit factor k_3. For the base metal with the LC orientation and for the weld metal, the values obtained in this study are higher than the codified values. Table 6 gives the results of the complementary analysis of the LC orientation data based on the sulfur content. It can be observed that low sulfur content (less than 0.005 %) gives much higher $J_{0.2}$ values.

Table 5. Results of the statistical analysis on $J_{0.2}$ values for carbon-manganese steels (base metal and weld).

$J_{0.2}$ (kJ/m^2) 16% fractile	**Base metal**			**Weld**
	RSE-M Code (*)	This study CL orientation	This study LC orientation	This study
T ≤ 140°C	92	79	118	163
T > 140°C	55	52	93	79

(*) The RSE-M Code values are based on CL orientation data. They can be used for LC orientation and for the welds.

Table 6. Results of the statistical analysis on $J_{0.2}$ values for carbon-manganese steels (base metal LC orientation).

$J_{0.2}$ (kJ/m^2) 16% fractile	**Base metal – LC orientation**	
	All temperatures	T > 140°C
S < 0.005 %	184	184
0.005 % ≤ S ≤ 0.015 %	114	102
0.015 % < S	80	66

4.4 Correlations between properties

Various correlations between properties have been examined in this study:

- tensile properties (ultimate stress and yield stress) at room temperature versus tensile properties around 300°C,
- KCV upper shelf energy (USE) versus sulfur content,
- fracture toughness properties ($J_{0.2}$ and dJ/da) around 300°C versus sulfur content,
- $J_{0.2}$ around 300°C versus KCV USE, for both base metal and weld metal.

Due to the lack of space, these correlations will not be recalled here (see Le Delliou (2007) for details).

4.5 Study of the strain aging phenomenon

In carbon steels, dynamic strain aging (DSA) is caused by interaction between dislocations and interstitial solutes (nitrogen and carbon) or solute pairs consisting of one interstitial and one solute atom (such as manganese-carbon and manganese-nitrogen). Indications of DSA are the presence of serrations on tensile curves, a maximum in flow stress with temperature and strain rate, reduction in ductility, and rapid strain hardening. The occurrence of DSA depends on the rate of solute diffusion and the dislocation velocity, which depend on temperature and strain rate. DSA is also associated with a minimum in fracture toughness properties at a temperature close to that corresponding to the maximum in flow stress: see for example Miglin (1985), Mohan (1988), Seok (1999), Yoon (1999), Kim (1995), Kim (1997), and Kim (2004).

A thesis study was conducted between 2004 and 2007 to better understand the effect of the strain aging on the fracture behavior of carbon-manganese steels (Belotteau 2006a, 2006b). A constitutive model based on the McCormick's model (1988) was developed to simulate the negative strain-rate sensitivity and discontinuous yielding (serrations and Lüders plateau). The parameters of this model were identified over a wide temperature range (20 to 350°C), using the experimental database developed on the TU48C #U634 steel (see section 4.1). This model was used to calculate CT specimens in order to examine plastic localizations in the vicinity of the crack tip. Classical variables which drive ductile damage, such as stress triaxiality, calculated with and without strain aging, were compared. Tests on round notched specimens with various radiuses were also conducted. The basis idea is to find a link between the plastic localization and the damage localization, which could accelerate the fracture process. Another thesis study was launched in 2008 to continue the work on this subject.

5 CONCLUSION

A project was conducted by EDF between 2004 and 2006 to improve RSE-M Code flaw evaluation. One task concerned the fracture toughness of austenitic stainless steels (mainly welds) and carbon-manganese steels (base metal and welds), typical of the primary and secondary piping of the French PWR. The main results of this task were described, i.e. the experimental material program, statistical analyses, correlations between properties and study of the strain aging phenomenon.

New fracture toughness data were developed on the steels under study, and added to the material databases. The statistical analyses of the $J_{0.2}$ parameter gave the following results for the 16% fractile:

- stainless steel welds: the un-aged SAW and SMAW values at T ≤ 100°C were slightly improved and specific values for GTAW were developed,
- carbon-manganese base metals and welds: the values for the base metals with LC orientation and for the welds are higher than the values for the base metals with CL orientation. Hence, specific values for base metal with LC orientation and for welds will be codified in the RSE-M Code.

Various correlations between fracture properties ($J_{0.2}$, dJ/da, KCV impact energy) or with the sulfur content were investigated. It appears that there is a lack of data, for example for carbon-manganese steels and CL orientation. Moreover, data taken from literature are sometimes dubious, for various reasons:

- lack of details on specimen orientation, chemical composition, test standard,
- values of $J_{0.2}$ (or J_{Ic}) calculated from unloading compliance tests with a large final propagation,
- use of non-standard specimens (without side-grooves, flattened, strongly sub-sized…).

Finally, a research work was conducted to better understand the effects of the strain aging on the fracture toughness properties of carbon steels.

On-going research is focused on the extension of the fracture toughness database for carbon-manganese steels (tests on main feedwater elbows retired from service) and the continuation of the work on the dynamic strain aging.

REFERENCES

Barthelet, B., and Faure, F., 1999, "Material properties for in-service inspection RSE-M Code flaw evaluation", Proc. SMIRT 15 Conference, Vol. III, paper D04/3, pp. 135-142

Belotteau, J., et al, 2006, "Mechanical behavior modeling in the presence of strain aging", Proc. 16th European Conference on Fracture (ECF16)

Belotteau, J., et al, 2006, "Strain aging and prediction of ductile fracture of C-Mn steels", Proc. 9th European Mechanics of Material Conference (EMMC9) *Local Approach to Fracture*, Moret-sur-Loing, France, pp. 187-192

Faidy, C., 2000, "RSE-M. A general presentation of the French codified flaw evaluation procedure", *Int. J. of Press. Vessels & Piping*, Vol. 77, pp. 919-927

Gavenda, D.J., et al, 1996, "Effects of thermal aging on fracture toughness and Charpy-impact strength of stainless steel pipe welds", NUREG/CR-6428 and ANL-95/47

Hiser, A.L., 1989, "Fracture toughness characterization of nuclear piping steels", NUREG/CR-5188 and MEA-2325

ISO 16269-6:2005, 2005, "Statistical interpretation of data – Part 6: Determination of statistical tolerance intervals"

Kim, I.S., and Tang, S.S., 1995, "Dynamic strain aging in SA508-class 3 pressure vessel steel", *Int. J. of Press. Vessels & Piping*., Vol. 22, pp. 123-129

Kim, J.W., and Kim, I.S., 1997, "Investigation of dynamic strain aging in SA106 Gr.C piping steel", *Nucl. Eng. Des.*, Vol. 172, pp. 49-59

Kim, K.C., et al, 2004, "Influences of dynamic strain aging on the J-R fracture characteristics of the ferritic steels for reactor cooling system", *Nucl. Eng. Des*., Vol. 228, pp. 151-159

Le Delliou, P., Sermage, J.P., and Barthelet, B., 2004, "Overview of flaw assessment methods in the RSE-M Code", Proc. ASME PVP Conference, Vol. 481, pp. 77-86

Le Delliou, P., et al, 2007, "Tensile and toughness properties of materials for the in-service inspection and flaw evaluation RSE-M Code", Trans. SMIRT 19 Conference, Paper # F04/1

McCormick, P.G., 1988, "Theory of flow localization due to dynamic strain aging", *Acta Met*., pp. 3061-3067

Miglin, M.T., et al, 1985, "Effects of strain aging in the unloading compliance J test", in *Elastic-Plastic Fracture Test Methods. The User's Experience*, ASTM STP 856, pp. 150-165

Mohan, R., and Marschall, C., 1988, "Cracking instabilities in a low-carbon steel susceptible to dynamic strain aging", *Acta Mater*., Vol. 46, pp. 1933-1948

RSE-M Code, 1997 Edition "*In Service Inspection Rules for the Mechanical Components of PWR Nuclear Power Islands"*, AFCEN

Seok, C.S., and Murty, K.L., 1999, "Effect of dynamic strain aging on mechanical and fracture properties of A516 Gr70 steel", *Int. J. of Press. Vessels & Piping*, Vol. 76, pp. 945-953

Yoon, J.H., et al, 1999, "Effects of loading rate and temperature on J-R fracture resistance of an A516 Gr.70 steel for nuclear piping", *Int. J. of Press. Vessels & Piping*, Vol. 76, pp. 663-670